Tornado Environments, Metrics, and Warnings: Lessons from a Ten-Year Climatology

ALEXANDRA K. ANDERSON-FREY * AND YVETTE P. RICHARDSON

The Pennsylvania State University, University Park, Pennsylvania.

ANDREW R. DEAN, RICHARD L. THOMPSON, AND BRYAN T. SMITH
Storm Prediction Center, Norman, Oklahoma

ABSTRACT

In this study, we highlight the regions of the environmental parameter space having low warning skill during particular times of day and times of year. This work makes use of the tornado warnings issued and tornado reports received across the continental United States between 2003 and 2013, coupled with warning verification data and proximity sounding data from the Rapid Update Cycle model, to create a 10.5-year tornado environment climatology and to evaluate tornado warning performance over this time as a function of tornado environment. We use a kernel density estimation approach to plot and compare distributions of tornado warnings and reports across two parameter spaces known for their ability to discriminate between various types of severe and non-severe weather: the most-unstable convective available potential energy vs. 0–6 km vector shear magnitude, and the height of the mixed-layer lifting condensation level vs. 0–1 km storm-relative helicity. We also group these reports and warnings by time of day, storm morphology, and time of year in order to highlight diurnal and seasonal differences in both warning skill and what characterizes a "typical" tornado environment.

1. Introduction

In order to produce timely and accurate tornado warnings, forecasters must synthesize a combination of factors, including their own understanding of the tornadic environment (incorporating a variety of conceptual models), as well as observations that are necessarily incomplete (e.g., radar velocities that are sampled significantly off the ground). By establishing and maintaining a detailed tornado climatology, and comparing the environmental distributions of tornado reports with those of tornado warnings, improvements can be made to the current understanding of and preparedness for tornadic storms.

During the period from 01 Jan 2003 through 30 Jun 2013, the probability of detection (POD, defined here as the fraction of tornado reports having positive leadtime) was 71%–that is, nearly three out of every four tornadoes had a warning issued ahead of time. In the same period, the false alarm ratio (FAR, defined here as the fraction of tornado warnings for which no associated tornado report is received; Barnes et al. 2009) was 77%–more than three out of every four tornado warnings were false alarms. In this work, we hope to ultimately take a "targeting approach" to the problem of improving tornado warning skill (i.e.,

reducing FAR without also reducing POD) by examining (1) how tornado warning skill varies as a function of tornado environment, and (2) how that skill-by-environment varies by additional factors such as the time of year or time of day. In this paper, we document the climatology of tornado events and warnings by environment.

2. Methods and Data

We examine tornado environments as defined by two different parameter spaces in this study (following, e.g., Anderson-Frey et al. 2012 and Schneider and Dean 2008). The first parameter space is most-unstable convective available potential energy (MUCAPE; the CAPE measured using the most unstable parcel in the lowest 300 mb) versus 0–6 km vector shear magnitude (SHR6), the combination of which has been shown (Brooks et al. 2003) to discriminate well between non-severe and severe storms. High-MUCAPE, high-SHR6 environments increase the potential for a supercellular storm. Note that in the following plots, MUCAPE is frequently replaced by the maximum updraft speed attained (under parcel theory assumptions) during the parcel's ascent, via $w_{max} = \sqrt{2 \times MUCAPE}$.

The second parameter space to be used is mixed-layer lifting condensation level (MLLCL) versus 0–1 km storm-relative helicity (SRH1; Markowski and Richardson 2014), the combination of which distinguishes fairly well

─────────
Corresponding author address: Alexandra K. Anderson-Frey, Department of Meteorology, The Pennsylvania State University, 406 Walker Building, University Park, PA 16801.
E-mail: aka145@psu.edu

Tornado Reports (2003-2013)
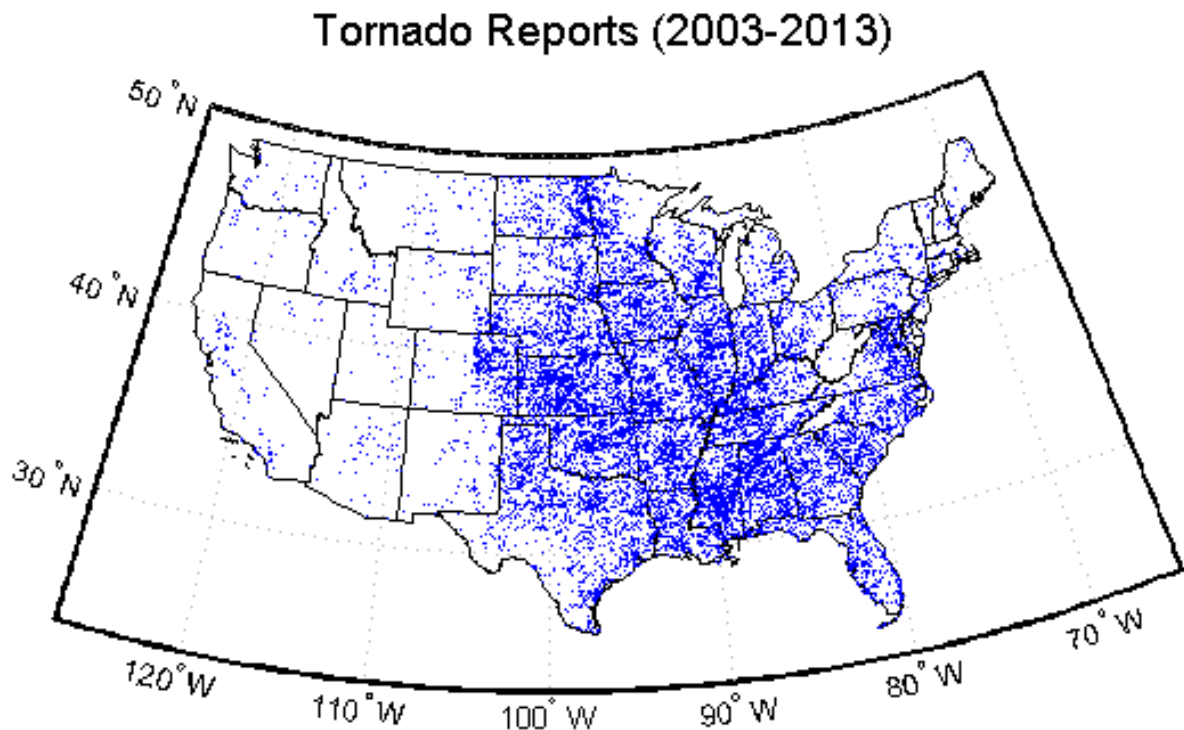
FIG. 1. Geographical distribution of tornado reports received between January 2003 and June 2013, inclusive.

between environments that support non-tornadic super-cells and environments that support significantly tornadic (i.e., EF2+) supercells (Thompson et al. 2012). High-SRH1, low-MLLCL environments increase the potential, given a supercell, for a significant tornado to occur.

The data used in this study draw from two major sources. The first is provided by archived mesoanalysis data (Dean et al. 2006) from the Storm Prediction Center (SPC). These proximity sounding data are obtained from the Rapid Update Cycle (RUC) model (Benjamin et al. 2002) for the data from Jan 2003–Apr 2012, af-ter which point the Rapid Refresh model (RAP) served as the basis for the SPC mesoanalysis data from May 2012–June 2013. By filtering county tornado segment data by maximum EF-scale on a 40-km grid hour, 12,090 tornado events were identified between 01 Jan 2003 and 30 Jun 2013, and were subsequently matched with the RUC/RAP proximity soundings. We also make use of the SPC's manual classification (Thompson et al. 2012; Smith et al. 2012) of each tornadic storm into one of three major

classes based on convective mode: quasi-linear convec-tive systems (QLCS), supercells, or disorganized convec-tion. The second dataset comes from the National Weather Service (NWS), and contains warning validation informa-tion for the 40,357 tornado warnings issued during the same period. Since a warning comprises an entire region rather than a point location, warnings were matched with RUC/RAP proximity soundings by selecting the grid point within the warning region that had the highest value of the significant tornado parameter (STP) contained within the warning box (Thompson et al. 2003, 2012). Figure 1 de-picts the geographical distribution of the tornado reports.

Instead of using one-dimensional box-and-whiskers plots (Thompson et al. 2012) or simple two-dimensional histograms (Schneider and Dean 2008, Anderson-Frey et al. 2012), we make use of a smoothing process known as kernel density estimation (KDE; Zucchini 2003, Peel and Wilson 2008), as illustrated in Fig. 2. Figure 2a de-picts a scatterplot of all tornado reports in the w_{max}-SHR6 parameter space, and Figure 2b corresponds to the KDE
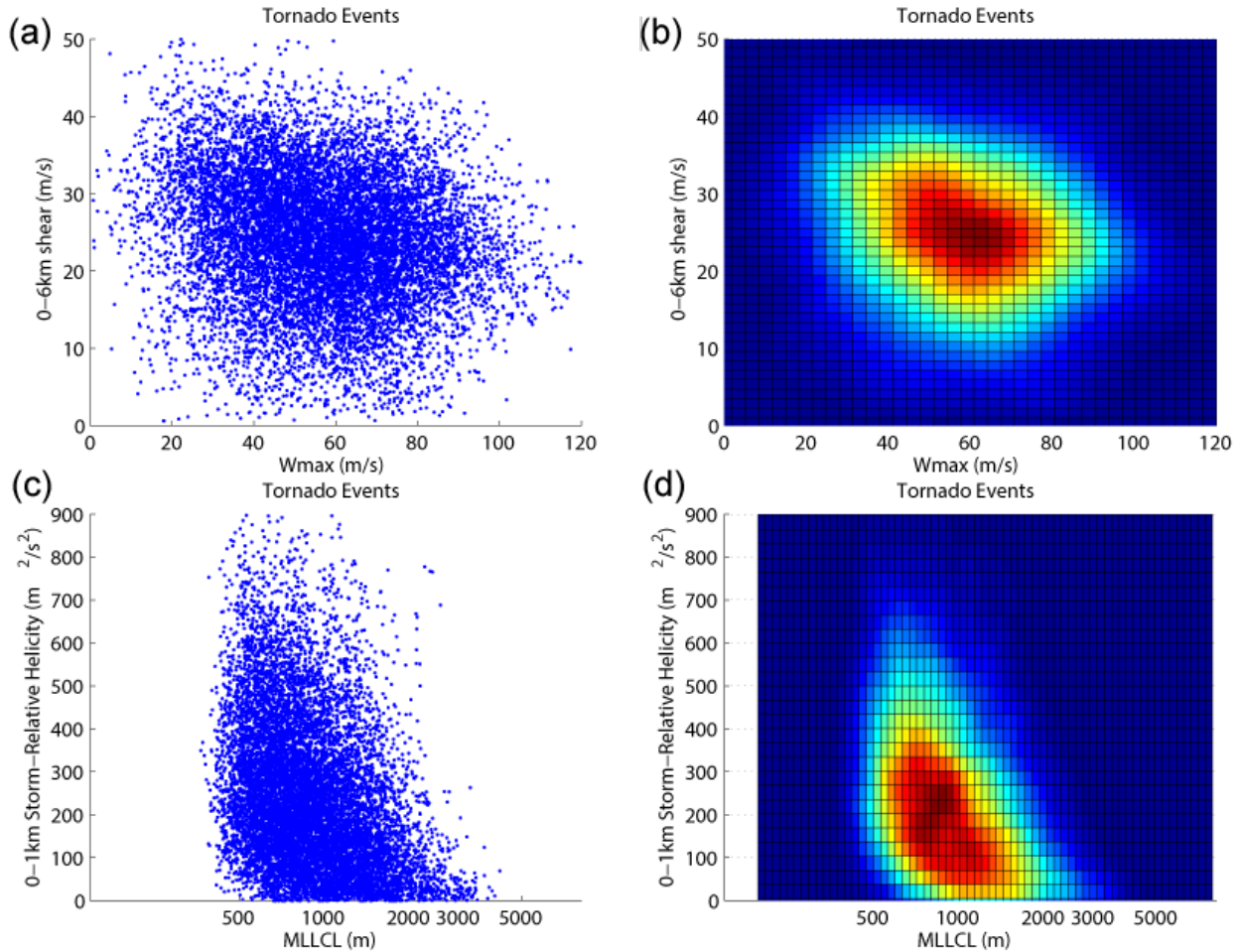
FIG. 2. Plots of 12,090 tornado events reported between 01 Jan 2003 and 30 Jun 2013. Scatterplots of all data are depicted in the (a) w_{max}-SHR6 and the (c) MLLCL-SRH1 parameter spaces. (b, d) Kernel density estimation (KDE) is used to smooth the data for the respective datasets. Warmer colors represent higher density.

smoothing of the entire dataset; note that it is considerably easier to identify the region of maximum density of tornado reports in the KDE plots than it is in the scatterplots. Similarly, Figs. 2c-d show the scatterplot and KDE plot, respectively, for the MLLCL-SRH1 parameter space.

3. Tornado Reports

From the plots in Fig. 2, it is clear that tornadoes occur in a wide variety of storm environments. The most common environments (i.e., the environments with the highest KDE values) in which reported tornadoes occur feature relatively large MUCAPE ($\sim$2000 J kg^{-1}), relatively strong SHR6 ($\sim$25 ms^{-1}), relatively low MLLCL heights ($\sim$800 m), and relatively strong SRH1 ($\sim$200m^{2}s^{-2}), agreeing well with tornadic environments as described in Brooks et al. (2003) and Thompson et al. (2003).

Further insight into "typical" climatological tornadic environments is gained by delving into some of the ad-

ditional categories provided by the dataset, such as storm mode, season, and time of day. Over all storm modes, only 21.2% of tornadoes occur at night (defined here as ranging from one hour after local sunset until sunrise). When considering only right-moving supercell (RMS) tornadoes, that percentage remains similar (20.9%), but when considering only QLCS tornadoes, we see that they tend to occur disproportionately at night (39.7%). In terms of seasonality, QLCS tornadoes comprise 29.7% of tornadoes in the winter months, versus only 6.3% of tornadoes in the summer months.

For the w_{max}-SHR6 parameter space, Fig. 3 splits the tornado reports into two categories: QLCS (Fig. 3b) and RMS (Fig. 3c). Fig. 3a is a repeat of Fig. 2b that depicts the KDE plot for all tornadoes in the dataset, for ease of comparison. Given that RMS storms comprise 70.1% of all tornado reports in this dataset, it is unsurprising that their distribution across this parameter space should look
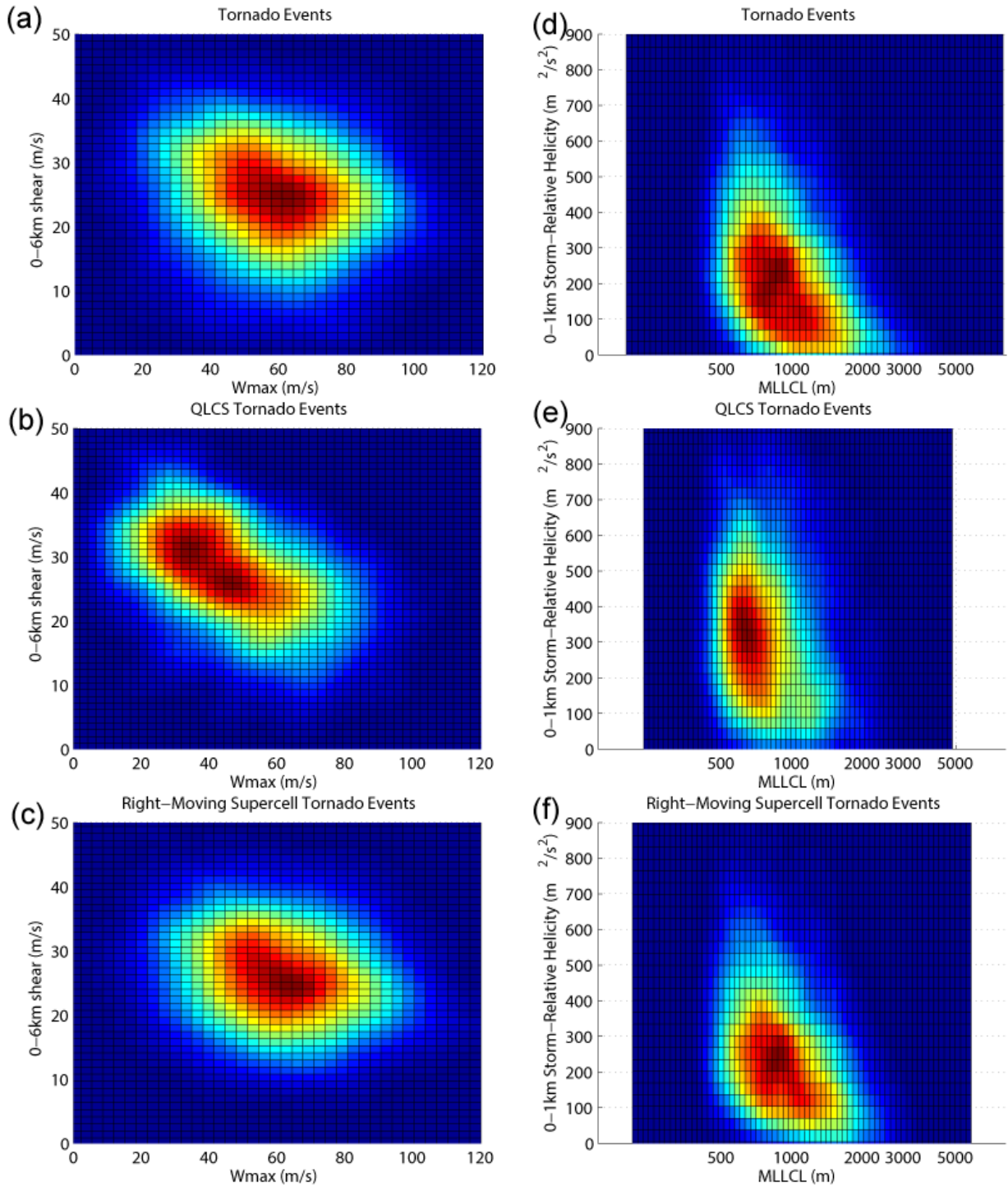
FIG. 3. KDE plot of tornado events in the (a-c) w_{max}-SHR6 parameter space and the (d-f) MLLCL-SRH1 parameter space. (a,d) KDE plot of all tornado events, (b,e) KDE plot of quasi-linear convective system (QLCS) tornado events, and (c,f) KDE plot of right-moving supercell (RMS) tornado events. Note that, while the resolutions of the axes are identical, the optimization algorithm for the KDE adjusts its plotting based on the range of values in each dataset. Since, for instance, the environments associated with QLCS storms cover a slightly narrower range of MLLCL values, the KDE plot will cover a narrower range in (e) than in (d).
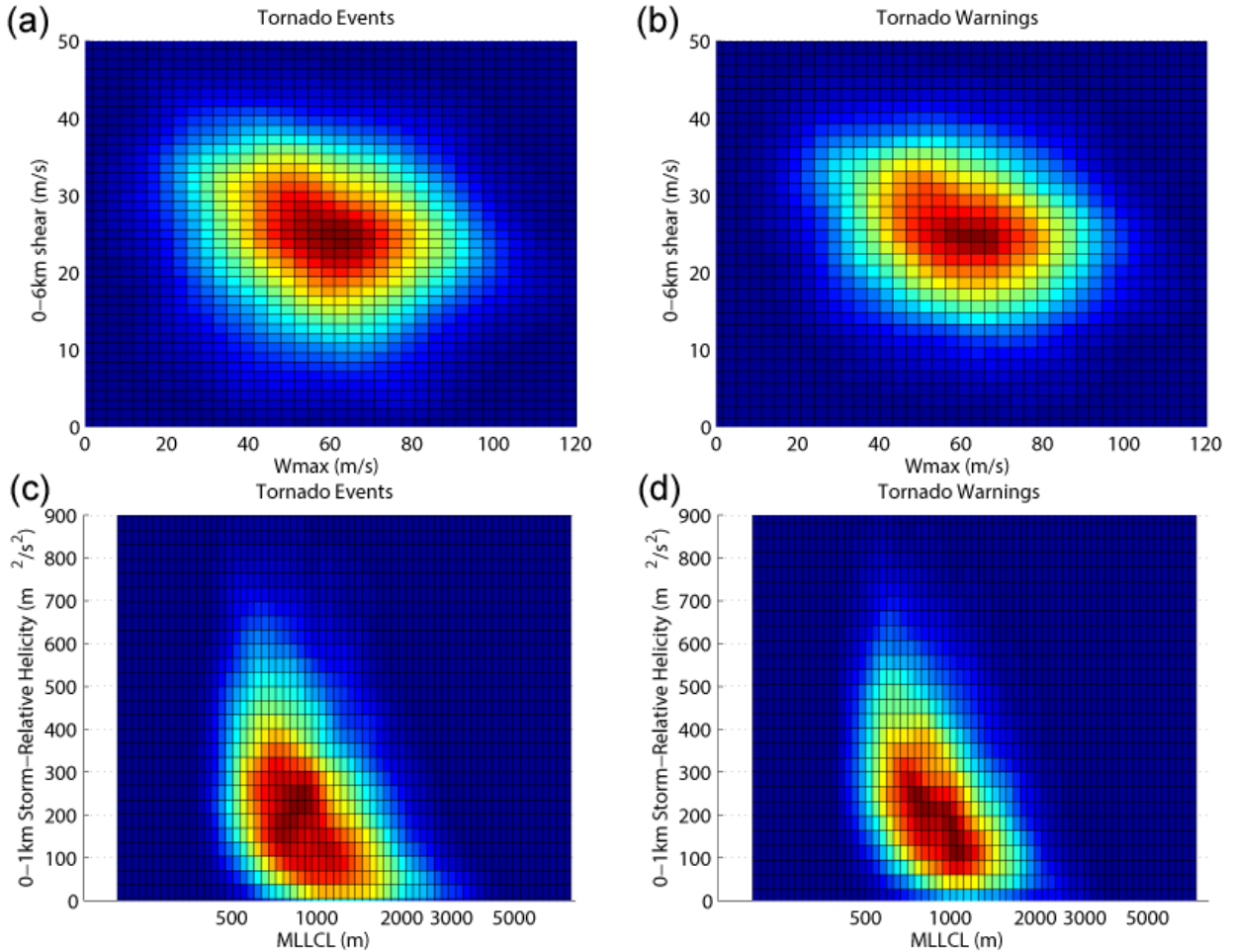
FIG. 4. Plots of (a, c) 12,090 tornado events and (b, d) 40,357 tornado warnings reported between 01 Jan 2003 and 30 Jun 2013. KDE plots of all data are depicted in the (a, b) w_{max}-SHR6 and the (c, d) MLLCL-SRH1 parameter spaces.

reasonably similar to that of the entire dataset. On the other hand, QLCS tornado events have their maximum occurrence at considerably lower w_{max} (and hence lower MUCAPE) values–unsurprising given that QLCS storms occur disproportionately at night and during the winter. While high-CAPE and high-shear tornado environments (e.g., Brooks et al. 2003) are seen as most favorable for severe convection to occur, it is worth noting that these QLCS storm environments, which are frequently characterized by low MUCAPE, account for an appreciable 11.8% of tornadoes in the continental U.S..

Figure 3 also depicts the total (Fig. 3d), QLCS (Fig. 3e), and RMS (Fig. 3f) KDE plots for the second parameter space, i.e., MLLCL-SRH1. Both QLCS and RMS environments are characterized by relatively high values (>150 m^2s^{-2}) of SRH1, but the QLCS storms display especially high values (centered at around 350 m^2s^{-2}). Also consistent with a higher percentage of nocturnal events,

QLCS tornadoes tend to diminish considerably in number as SRH1 decreases below 50 m^2s^{-2}.

4. Tornado Warnings

While it is impractical to create a similarly involved manual classification database of storm mode for the 40,357 tornado warnings that comprise the second part of this dataset, there are indeed time-of-day and time-of-year data, to be explored in the following section.

Fig. 4 displays tornado reports (Figs. 4a and c; cf. Fig. 2) and tornado warnings (Figs. 4b and d) for the entire dataset in each of the two parameter spaces. For the most part, the distributions of tornado warnings and reports match extremely well for the w_{max}-SHR6 parameter space (Fig. 4a-b); that is, the tornado warnings are being issued for the same part of the parameter space as the reported tornadoes. There is a slight difference in the MLLCL-SRH1 parameter space: the tornado warnings (Fig. 4d) have a relatively firm cutoff for low values of
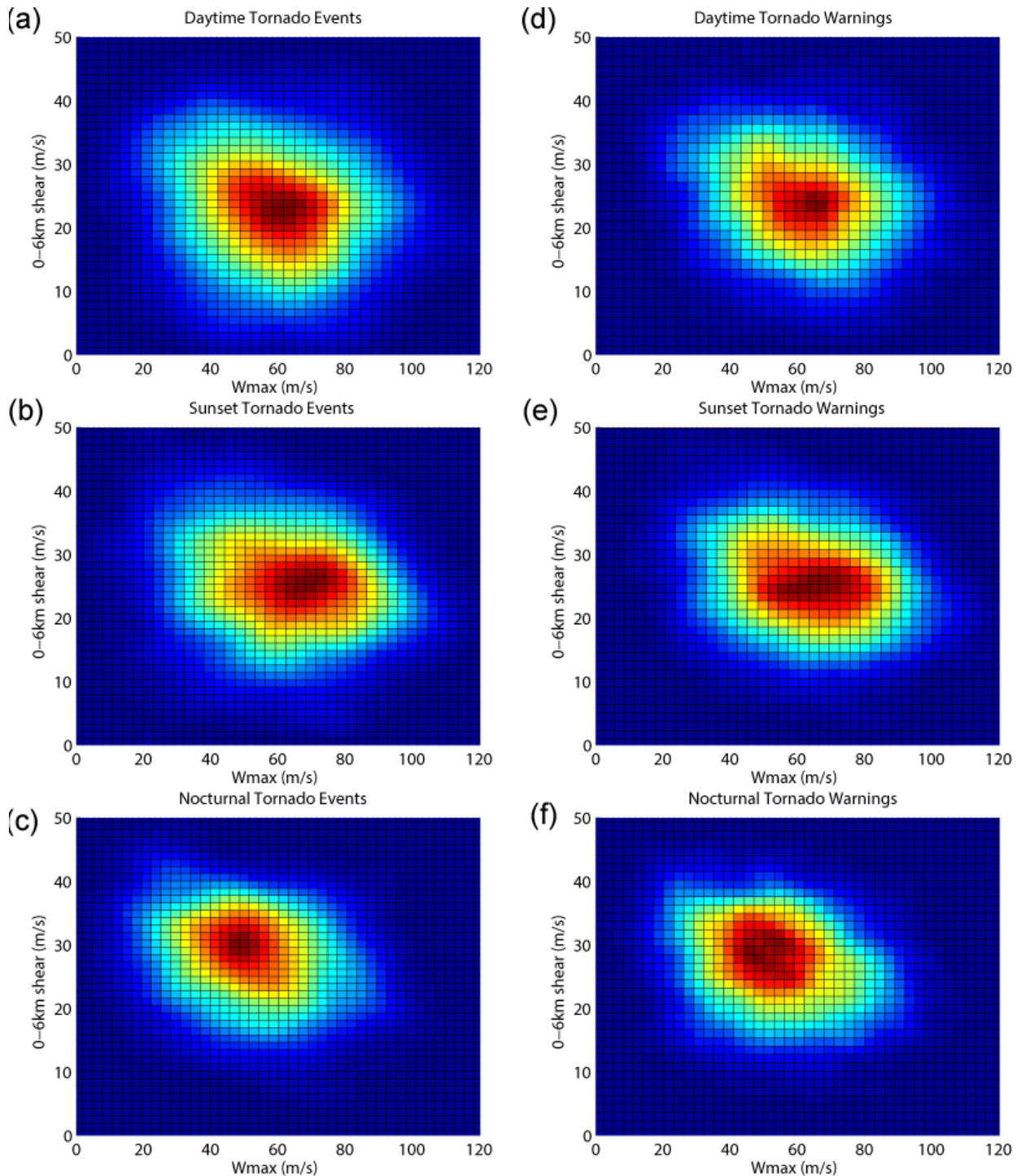
FIG. 5. KDE plot in the w_{max}-SHR6 parameter space of tornado reports (a–c) and tornado warnings (d–f), separated by time of day. The daytime category (a, d) consists of all tornadoes occurring between sunrise and two hours prior to local sunset. The sunset category (b, e) includes all tornadoes occurring between two hours prior to local sunset and one hour after local sunset. Finally, the nocturnal category (c, f) features tornadoes occurring between one hour after local sunset and sunrise.

SRH1 when compared with the tornado reports (Fig. 4c). However, when these (E)F0 tornadoes are removed from the tornado report dataset (not shown), the two distributions in this parameter space become more aligned, indi-
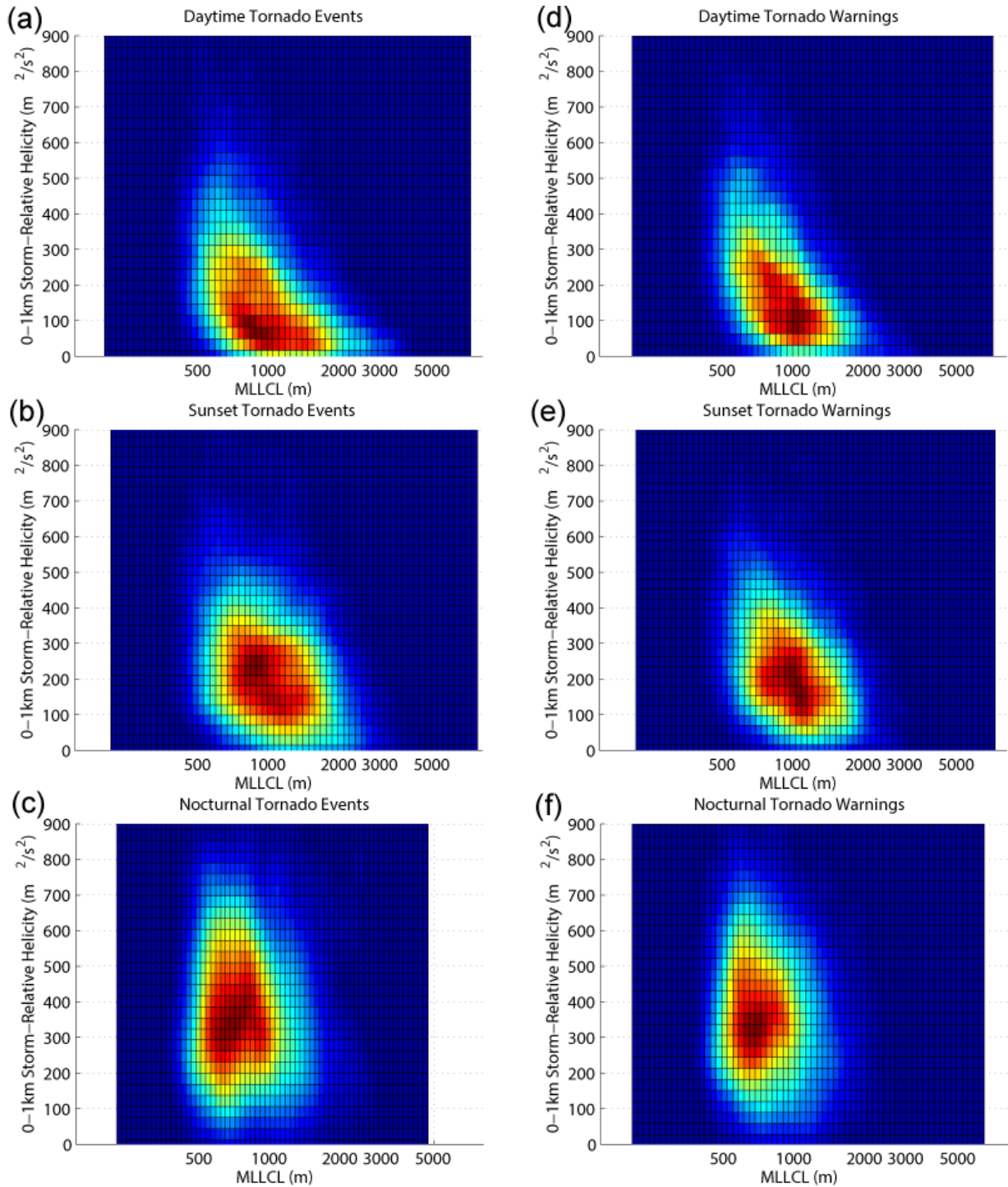
FIG. 6. As in Fig. 5, but for the MLLCL-SRH1 parameter space.

cating the difficulty in issuing warnings for (E)F0 tornadoes, which are frequently short-lived, do minimal damage, and occur under marginal environmental conditions.

a. Time of Day

We might expect the tornado environments to vary somewhat by time of day, given the diurnal evolution of
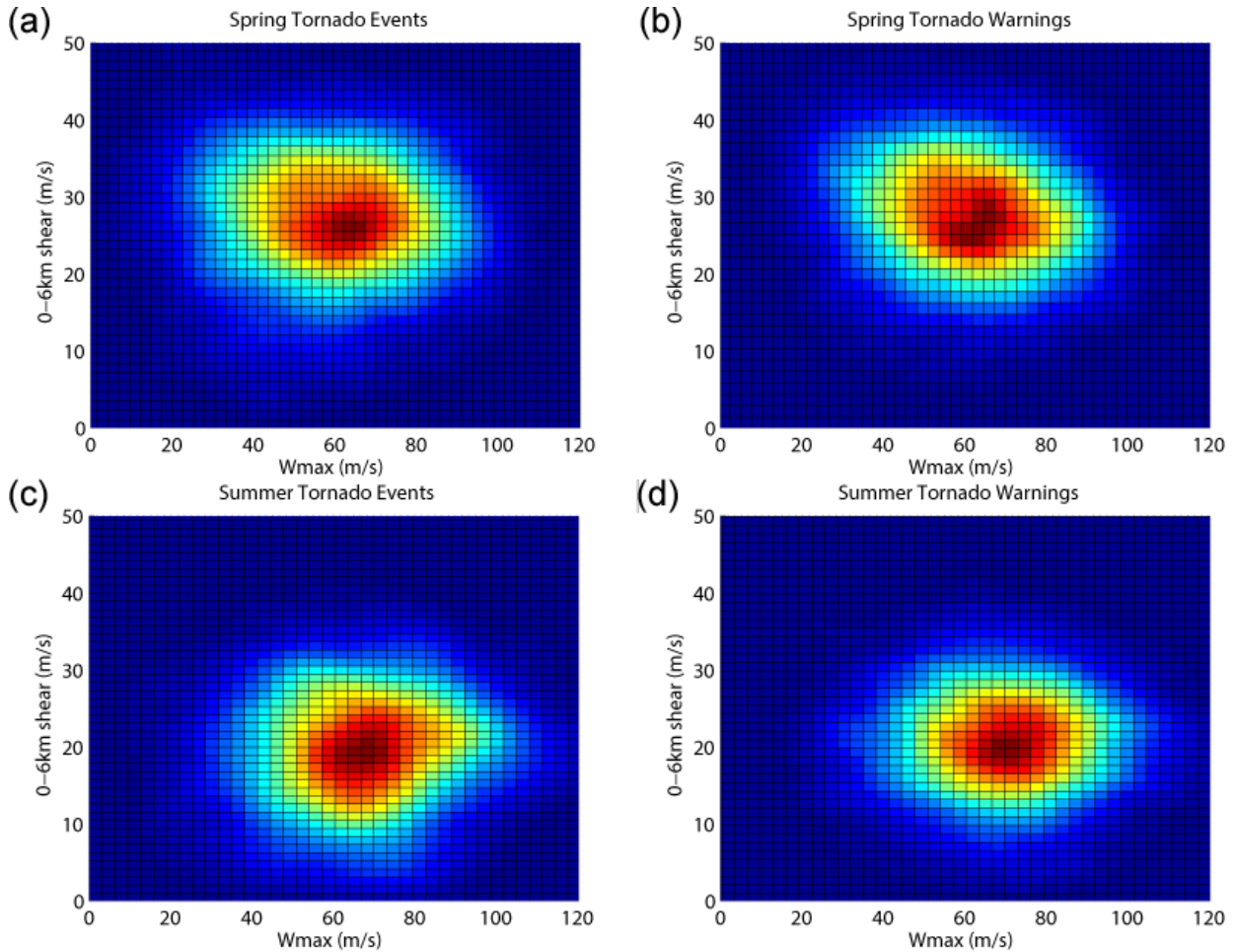
FIG. 7. KDE plots in the w_{max}-SHR6 parameter space of tornado reports (a, c) and tornado warnings (b, d), separated by time of year. Spring (a, b) is MAM and Summer (c, d) is JJA.

the lowest levels in the atmosphere. Indeed, even significant (EF2+) nocturnal tornadoes can sometimes thrive in storm environments that might regularly be deemed thermodynamically unfavorable for tornadogenesis, with marginal thermodynamic instability perhaps offset by higher storm-relative helicity owing to the presence of a nocturnal low-level jet (Kis and Straka 2010). To examine these relationships, we split the dataset into three bins based on time-of-day: day (ranging from sunrise until two hours before local sunset), sunset (ranging from two hours before local sunset until one hour after local sunset), and night (ranging from one hour after local sunset until sunrise). The presence of the "sunset" category is intended as a buffer period during the transition from a convective boundary layer to a stable boundary layer.

Nocturnal tornadoes, based on the above definition, correspond to only 21.2% of the entire dataset, but comprise 44.1% of the tornadoes that occur during the winter months. They also comprise nearly half (49.7%) of all tor-

nadoes in the Southern region of the United States. Wintertime nocturnal tornadoes in the Southeastern United States, particularly QLCS storms in coastal regions, are well-documented in previous studies (e.g., Fike 1993 and Guyer et al. 2006).

In Fig. 5a-c, the w_{max}-SHR6 parameter space diagrams for tornado events split into (a) daytime, (b) sunset, and (c) nocturnal tornadoes are depicted. During the sunset period (Fig. 5b), the maximum density of tornado events occurs at the highest values of MUCAPE, presumably owing to the timing of the typical diurnal maximum in surface temperature. On the other hand, nocturnal tornado environments are predictably characterized by lower MUCAPE. Although there is a great deal of overlap between the distributions of the three categories when it comes to SHR6 values, nocturnal tornado events display slightly stronger SHR6.

The tornado warnings depicted in Fig. 5d-f are plotted for comparison with the tornado reports. Although
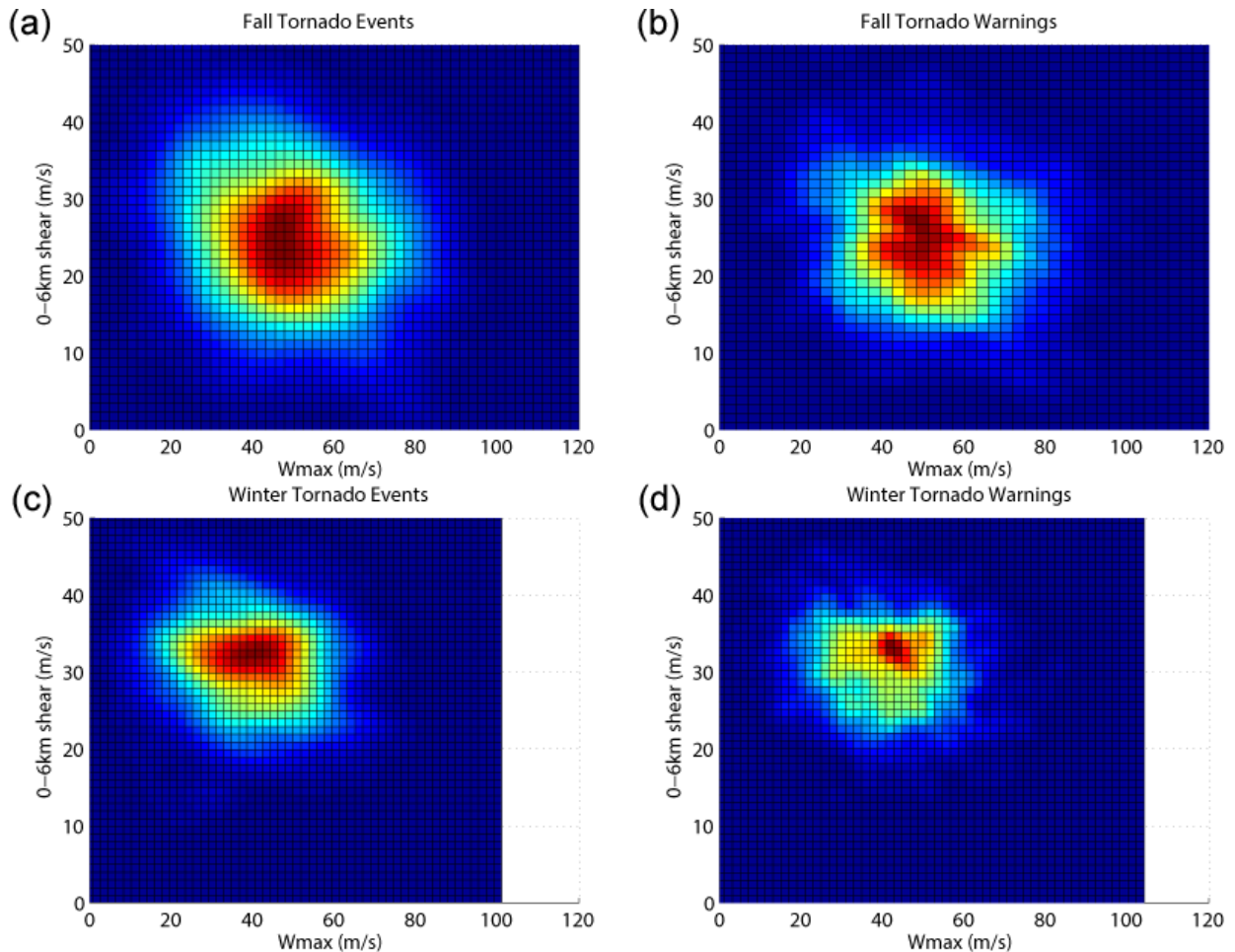
FIG. 8. As in Fig. 7, but for fall (a, b; SON) and winter (c, d; DJF).

there are some minor differences between the event and warning distributions, such as the sunset warnings' slight overemphasis of the lower-MUCAPE environment when compared with the sunset tornado events, overall tornado warnings are being issued for the same part of the parameter space as tornado events when split according to time of day.

Figure 6 depicts the tornado reports and warnings for the MLLCL-SRH1 parameter space. For daytime tornado warnings (Fig. 6d), there is a similar issue to that observed in the dataset as a whole: that is, the highest KDE values occur at stronger values of SRH1 than the highest KDE values for tornado reports. When the marginal (E)F0 tornadoes are removed, however, the discrepancy vanishes.

b. Time of year

To study seasonal influences on the tornado warning and report climatologies, we use the standard meteorological definitions of spring as March, April, and May

(MAM); summer as June, July, and August (JJA); fall as September, October, and November (SON); and winter as December, January, and February (DJF). Tornadoes that occur in the winter also tend to occur somewhat disproportionately at night, particularly in the Southern region of the United States. QLCS tornadoes also comprise a larger fraction of tornadoes in the winter than during the rest of the year; winter tornadoes comprise only 8.7% of the entire tornado database, but they comprise 22.1% of the QLCS tornadoes. In the summer, (E)F0 tornadoes comprise a larger fraction of the total number of tornadoes than for any of the other seasons; (E)F0 tornadoes comprise 56.5% of the entire dataset, but that number rises to 69.9% when considering only the tornadoes that occur during the summer months.

Figs. 7 (spring, summer) and 8 (fall, winter) depict the tornado reports and warnings in the w_{max}-SHR6 parameter space, separated by season. In the spring, tornado report environments (Fig. 7a) tend to reflect the more "textbook" high-MUCAPE, high-SHR6 environments that are
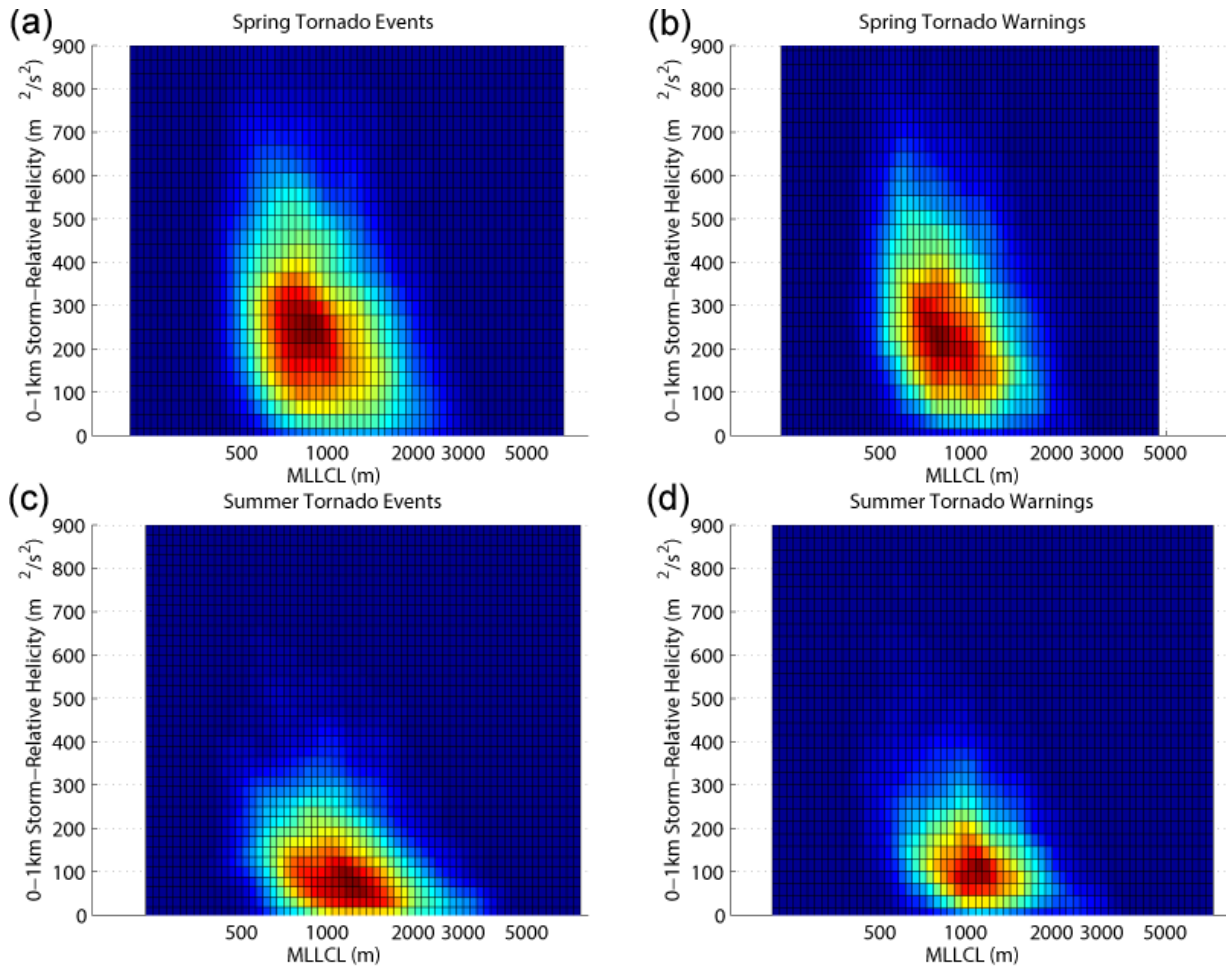
FIG. 9. As in Fig. 7, but for the MLLCL-SRH1 parameter space.

common over the Great Plains during tornadic outbreaks. During the summer (Fig. 7c), tornadic environments shift to lower-SHR6, slightly higher-MUCAPE parts of the parameter space, due in part to the disproportionate presence of marginal (E)F0 tornadoes during this season. Fall (Fig. 8a) and especially winter (Fig. 8c) are characterized by stronger SRH6 and smaller MUCAPE, which is unsurprising given the seasonal increase in baroclinity and decrease in instability.

The tornado warnings (Fig. 7b, d and Fig. 8b, d) tend to reflect these tendencies well, especially in the spring, summer, and fall. In the winter (Fig. 8c-d), there is a small discrepancy: tornado warnings tend to be centered for somewhat higher-MUCAPE values than the reported tornadoes, which perhaps indicates a poorer understanding of the high-SHR6, low-MUCAPE part of the parameter space and the nocturnal QLCS storms that often occur in those environments.

Similarly, Figs. 9 and 10 depict the storm environments in the MLLCL-SRH1 parameter space for each of the four seasons. In the summer (Fig. 9c), environments are characterized by relatively high MLLCL and relatively low SRH1, once again highlighting the strong presence of marginal tornadoes during this season. In the fall, spring, and especially the winter (Fig. 10d), we see higher values of SRH1 and lower values of MLLCL.

The tornado warnings (Fig. 9b, d and Fig. 10b, d) show generally good agreement with the tornado reports. The same issue that occurs with tornado report environments as a whole is most apparent in summer (Fig. 9c-d): tornado warnings are generally occurring for somewhat less marginal parts of the parameter space when compared with the tornado reports, since warnings are (and perhaps should be) issued less frequently for (E)F0 tornadoes. For spring warnings (Fig. 9a-b), the distribution matches almost perfectly with the distribution of tornado reports. Fall (Fig. 10a-b) and winter (Fig. 10c-d) tornado warnings share similarly high skill when it comes to focusing on the correct region of the parameter space. However, warning environments with the highest KDE tend to be relatively
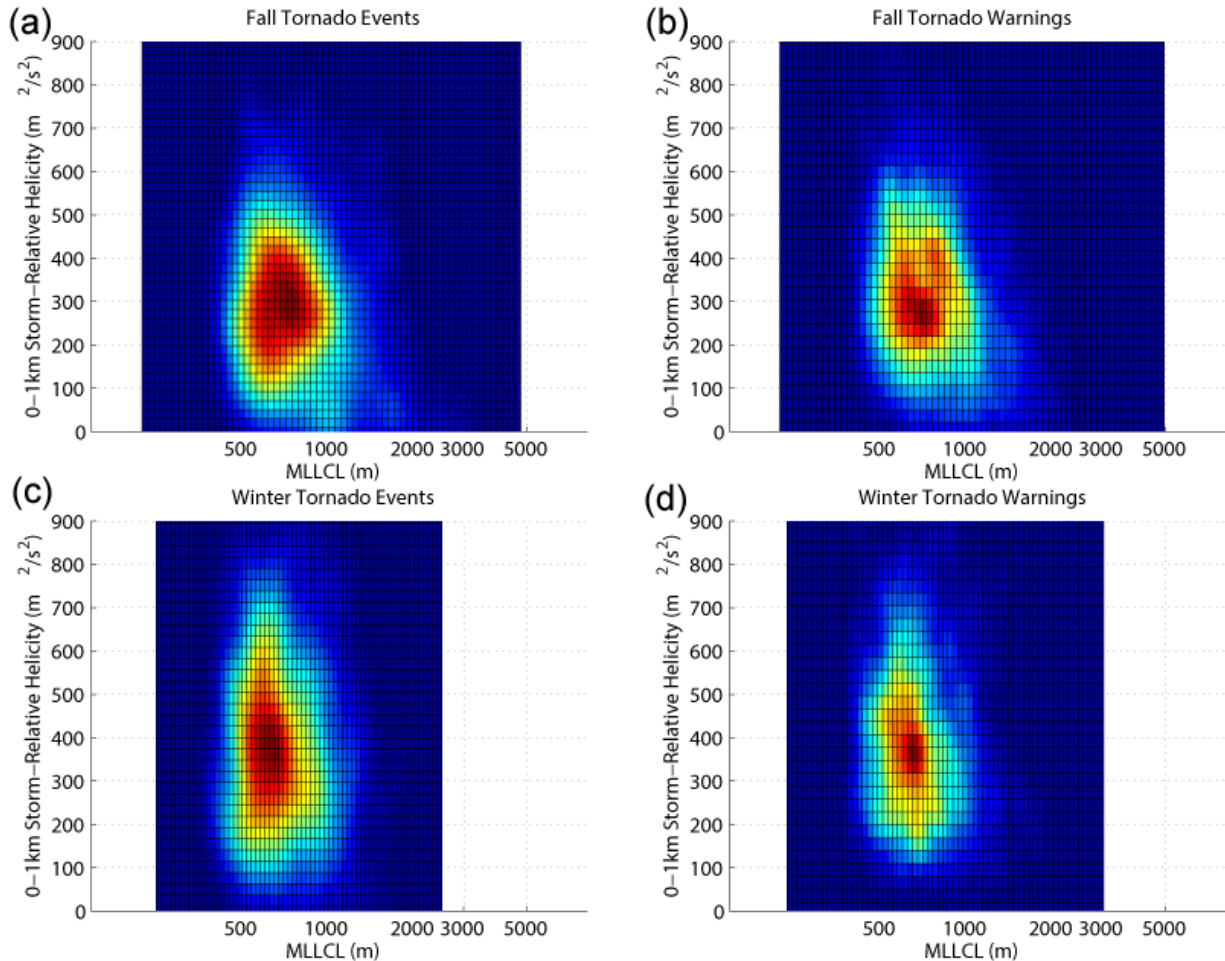
FIG. 10. As in Fig. 8, but for the MLLCL-SRH1 parameter space.

narrow when compared with high-KDE environments in the report database, suggesting that tornado warnings are focused on a smaller region of the parameter space, with less variability than the events. Perhaps warnings in the fall and the winter tend to be issued based on an overly restrictive set of environmental guidelines compared to the spring or the summer.

5. Summary and Conclusions

This work shows significant overlap between the environmental parameter spaces corresponding to the highest density of tornado events and tornado warnings, even when the data are split by time of day and time of year. Future work includes separating the data into additional categories such as observed mesocyclone strength, tornado intensity (i.e., EF-scale rating), and geographical distribution, in order to build a tornado report and warning climatology that takes into account additional factors that have a strong impact on the regions of the parameter space that are especially favorable for tornadogenesis and that show considerable forecast skill or lack thereof.

Another factor that has been shown to impact forecast performance is the order of tornadoes, i.e., whether or not a tornado is the first to be produced by a given storm system (Brotzge and Erickson 2009). We expect POD to be especially low for the first tornado in a given system, and FAR to be especially high for the last tornado in a given system. This hypothesis will be tested.

The ultimate goal is to identify portions of the parameter space having the lowest forecast skill and create an improved paradigm for tornado forecasting based on an improved understanding of tornadogenesis in those environments. These operationally oriented approaches to the problem of tornado forecasting will, in turn, result in more complete and comprehensive tornado climatologies, providing an invaluable contribution to researchers' conceptual models of tornadogenesis.

References

Anderson-Frey, A., Y. Richardson, and A. Dean, 2012: Preliminary investigation of tornado warning skill by environment. Preprints, *26th Conf. on Severe Local Storms*, Nashville, TN, AMS, P8.119.

Barnes, L., D. Schultz, E. Gruntfest, M. Hayden, and C. Benight, 2009: Corrigendum: False Alarm Rate or False Alarm Ratio? *Wea. Forecasting*, **24**, 1452–1454.

Benjamin, S., and Coauthors, 2002: RUC20–The 20-km version of the Rapid Update Cycle, NWS tech. proc. bull. 490. 30 pp.

Brooks, H., J. Lee, and J. Craven, 2003: The spatial distribution of severe thunderstorm and tornado environments from global reanalysis data. *Atmos. Res.*, **67–68**, 73–94.

Brotzge, J., and S. Erickson, 2009: NWS tornado warnings with zero or negative lead times. *Wea. Forecasting*, **24**, 140–154.

Dean, A., R. Schneider, and J. Schaefer, 2006: Development of a comprehensive severe weather forecast verification system at the Storm Prediction Center. Preprints, *23rd Conf. on Severe Local Storms*, St. Louis, MO, AMS.

Fike, P., 1993: A climatology of nocturnal severe local storms outbreaks. Preprints, *17th Conf. on Severe Local Storms*, St. Louis, MO, AMS, 10–14.

Guyer, J., D. Imy, A. Kis, and K. Venable, 2006: Cool season significant (F2-F5) tornadoes in the Gulf Coast states. Preprints, *23rd Conf. on Severe Local Storms*, St. Louis, MO, AMS, 4.2.

Kis, A., and J. Straka, 2010: Nocturnal tornado climatology. *Wea. Forecasting*, **25**, 545–561.

Markowski, P., and Y. Richardson, 2014: The influence of environmental low-level shear and cold pools on tornadogenesis: Insights from idealized simulations. *J. Atmos. Sci.*, **71**, 243–275.

Peel, S., and L. Wilson, 2008: Modeling the distribution of precipitation forecasts from the Canadian Ensemble Prediction System using kernel density estimation. *Wea. Forecasting*, **23**, 575–595.

Schneider, R., and A. Dean, 2008: A comprehensive 5-year severe storm environment climatology for the continental United States. Preprints, *24th Conf. on Severe Local Storms*, Savannah, GA, AMS.

Smith, B., R. Thompson, J. Grams, C. Broyles, and H. Brooks, 2012: Convective modes for significant severe thunderstorms in the contiguous United States. Part I: Storm classification and climatology. *Wea. Forecasting*, **27**, 1114–1135.

Thompson, R., R. Edwards, J. Hart, K. Elmore, and P. Markowski, 2003: Close proximity soundings within supercell environments obtained from the Rapid Update Cycle. *Wea. Forecasting*, **18**, 1243–1261.

Thompson, R., B. Smith, J. Grams, A. Dean, and C. Broyles, 2012: Convective modes for significant severe thunderstorms in the contiguous United States. Part II: Supercell and QLCS tornado environments. *Wea. Forecasting*, **27**, 1136–1154.

Zucchini, W., 2003: Course notes, Econ616, Temple University. [Available online at http://isc.temple.edu/economics/Econ616/Kernel/ast_part1.pdf].